Chapter 7

Susceptibility of Group-IV and III-V Semiconductor-Based Electronics to Atmospheric Neutrons Explored by Geant4 Numerical Simulations

Daniela Munteanu and Jean-Luc Autran

Additional information is available at the end of the chapter

http://dx.doi.org/10.5772/intechopen.71528

Abstract

New semiconductor materials are envisaged in numerous high-performance applications for which the expected device or circuit performances cannot be achieved with silicon. In this context of growing use of new and specific semiconductors, the question of their susceptibility to natural radiation, primarily to atmospheric neutrons, is posed for high-reliability-level application domains. This numerical simulation work precisely examines nuclear events resulting from the interaction of atmospheric neutrons at the terrestrial level with a target layer composed of various group-IV and III-V semiconductor materials including silicon, germanium, silicon carbide, carbon-diamond, gallium arsenide, and gallium nitride materials. Using extensive Geant4 simulations and in-depth data analysis, this study provides an accurate and fine comparison between the neutron interaction responses of these different semiconductors in terms of nuclear processes, recoil products, secondary ion production, and fragment energy distributions. Implications of these results on the rate of single-event transient effects at the device or circuit level are also discussed.

Keywords: terrestrial cosmic rays, atmospheric neutrons, neutron-semiconductor interactions, group-IV semiconductors, III-V semiconductors, nuclear reactions, Geant4, numerical simulations, radiation effects on electronics, single-event effects

1. Introduction

Modern electronics and optoelectronics are increasingly based on specific semiconductor materials other than silicon, including some elemental or compound semiconductors like germanium, silicon-germanium, and silicon carbide (group-IV) and III-V alloys [1]. These new materials are

attracting strong interest because of their better electronic transport, optical, or high-frequency properties than Si; they can be envisaged in numerous high-performance applications (e.g., "More than Moore" microelectronics and beyond CMOS, extreme environments, high temperatures, or high-speed electronics) for which the expected device or circuit performances cannot be achieved with silicon. In such a context of growing use of new and specific semiconductors, the question of their susceptibility to natural radiation, primarily to atmospheric neutrons at ground level, is posed for high-reliability-level application domains. A special attention should be particularly paid to low-bandgap materials (Ge and most of III-V materials), envisaged as channel replacement for MOSFETs and steep switching tunnel FETs for low voltage application [2], due to their low ionization energy susceptible to amplify charge generation from sea-level neutron radiation.

Following a methodology previously developed for the study of neutron-silicon interactions [3], the present work precisely examines nuclear events resulting from the interaction of atmospheric neutrons at the terrestrial level with a target layer composed of Si, Ge, SiC, C (diamond), GaAs, and GaN materials and representative of the whole sensitive volume of a typical integrated circuit. To perform this task, we constructed using the Geant4 toolkit [4, 5] a specific source of atmospheric neutrons and compiled large databases of neutron-semiconductor interaction events corresponding to tens of thousands of nuclear reactions. Details of these simulations and database compilation are given in Section 2. Section 3 presents a detailed analysis of obtained databases in terms of nuclear processes, recoil products, secondary ion production, and fragment energy distributions. Finally, Section 4 discusses the implications of these results on the rate of single-event transient effects at the device or circuit level.

2. Simulation details

2.1. Semiconductor materials

For the purpose of this study, we considered different group-IV and III-V semiconductor materials including silicon, germanium, silicon carbide, carbon-diamond, gallium arsenide, and gallium nitride materials. **Table 1** summarizes the main physical and atomic properties of these materials [6] notably in terms of bandgap value, bulk density, average energy for creation of an electron–hole pair and energy threshold to deposit 1.8 fC in the considered material. This last quantity corresponds to a silicon recoil nucleus in silicon material with a kinetic energy of 40 keV, considered in [3] as the lowest deposited charge susceptible to induce a soft error in a bulk 65 nm SRAM memory. For standardization purpose and comparison with results presented in [2], we adopted here the same lowest deposited charge (1.8 fC corresponds to 11,250 electrons) that leads to $E_{th} = 11{,}250 \times E_{eh}$. In other words, all neutron-induced products with energies below E_{th} will not be considered in the databases (see paragraph 2.3).

2.2. Atmospheric source of neutrons

The different semiconductor materials given in **Table 1** have been irradiated with atmospheric neutrons in Geant4 simulations described below (paragraph 2.3) and schematically represented in the inset of **Figure 1**. For memory, the interaction of primary cosmic rays with the Earth's top

Properties (300 K)	Si	Ge	C (diamond)	4H–SiC	GaN	GaAs
Semiconductor group	IV				III-V	
Atomic number	14	32	6	14/6	31/7	31/33
Bandgap (eV)	1.124	0.661	5.47	3.23	3.39	1.424
Structure	Diamond (cubic)			Wurtzite (hexagonal)		Zinc Blende (cubic)
Lattice constant (Å)	5.43	5.65	3.567	3.73 10.053	3.186 5.186	5.653
Density (g/cm^3)	2.329	5.3267	3.515	3.21	6.10	5.32
Atoms (/cm^3)	5.0×10^{22}	4.42×10^{22}	1.76×10^{23}	5.0×10^{22}	8.7×10^{22}	4.5×10^{22}
Average energy (E_{eh}) for creation of an electron-hole pair (eV)	3.6	2.9	12	7.8	8.9	4.8
Energy threshold (E_{th}) to deposit 1.8 fC (keV)	40	33	135	58	100	47

Table 1. Main structural, atomic, and electronic properties of the different group-IV and III-V semiconductor materials considered in the present study. (Data partially from Ref. [6]).

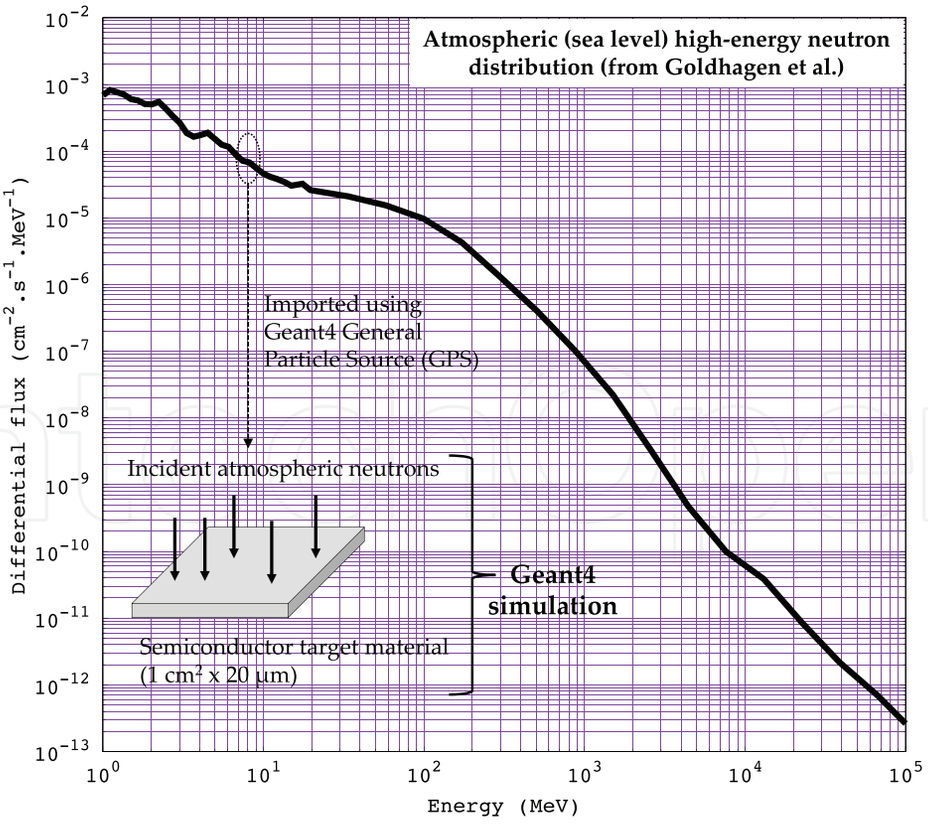

Figure 1. Differential flux of cosmic-ray induced high-energy neutrons as measured by Gordon and Goldhagen et al. using a multielement Bonner sphere spectrometer on the roof of the IBM T. J. Watson Research Center in Yorktown Heights, NY [6]. *Inset*: Schematic representation of the neutron irradiation simulated using Geant4 in this work.

atmosphere is at the origin of atmospheric showers that produce secondary particles down to the sea level. After muons, the next most abundant secondary particles at the sea level are neutrons. High-energy neutrons (typically above 1 MeV) represent by far the main threat to electronics at the ground level because these particles being not charged are very invasive and can penetrate deeply in circuit materials where they can interact with atoms to produce charged products (recoil nuclei or secondary ions).

To emulate the atmospheric neutron source, the differential flux of cosmic-ray induced high-energy neutrons measured by Gordon and Goldhagen et al. in Yorktown Heights [7] has been considered as the reference input spectrum [8]. This distribution, shown in **Figure 1**, was imported in the Geant4 general particle source (GPS) library [9] to randomly generate incident neutrons mimicking the natural sea-level neutron background.

2.3. Geant4 options, models, and simulation runs

The neutron interaction databases for the different semiconductor materials listed in **Table 1** have been computed in this work using Geant4 version 4.9.4 patch 01. The list of physical processes employed in simulation is based on the standard package of physics lists QGSP_BIC_HP [10]. Concerning the hadronic interactions, in QGSP group of physics lists, the quark gluon string model is applied for high-energy (above ~12 GeV) interactions of protons, neutrons, pions, kaons, and nuclei. The high-energy interaction creates an excited nucleus, which is passed to the precompound model describing the nuclear de-excitation. Nuclear capture of negative particles is simulated within the chiral invariant phase space (CHIPS) model. QGSP_BIC_HP list includes binary cascade for primary protons and neutrons with energies below ~10 GeV and also uses binary light ion cascade for inelastic interaction of ions up to few GeV/nucleons with matter. The complete list of the Geant4 classes that we considered for our neutron simulations is summarized in **Table 2**.

For each semiconductor target, a simulation run consists in the generation of 100 millions (10^8) of primary incident neutrons on a 20-μm-thick material layer perpendicular to its surface (1 cm^2).

Neutron process	Energy	Geant4 model	Dataset
Elastic	< 20 MeV	G4NeutronHPElastic	G4NeutronHPElasticData
	> 20 MeV	G4LElastic	-
Inelastic	< 20 MeV	G4NeutronHPInelastic	G4NeutronHPInelasticData
	[20 MeV, 10 GeV]	G4BinaryCascade	-
	[10 GeV, 25 GeV]	G4LENeutronInelastic QGSP	-
	[12 GeV, 100 TeV]		-
Fission	< 20 MeV	G4NeutronHPFission G4LFission	G4NeutronHPFissionData
	> 20 MeV		-
Capture	< 20 MeV	G4NeutronHPCapture G4LCapture	G4NeutronHPCaptureData -
	> 20 MeV		

Table 2. List of the different Geant4 classes considered in the present simulation flow for the description of neutron-matter interactions.

http://dx.doi.org/10.5772/intechopen.71528

All particles characterized by tiny (i.e., insignificant) ionizing properties and thus negligible impact on electronics in terms of electron-pair generation and single events have been excluded from the simulation. Consequently, the computed databases exclude electrons, positrons, gamma photons, pions, and mesons and only contain protons, alpha particles, and ionizing products with $Z > 2$.

The target dimensions have been chosen to match the typical dimensions of the sensitive volume of an integrated circuit. In particular, the thickness has been fixed to 20 μm because the electrical charge generated by a reaction product beyond 20 μm would not drift or diffuse to the active area (i.e., the sensitive region of the circuit located close to the semiconductor surface) and, consequently, would not play any role in the occurrence of single events.

3. Simulation results

3.1. Main characteristics of the databases

An example of the computed databases is given in **Table 3** for a target composed of GaAs material and subjected to atmospheric neutron irradiation. As illustrated in this sample composed of nine events, each neutron-interaction event is described in two or several successive lines: the first line gives the event number, the energy of the incident neutron at the origin of the event, the Cartesian coordinates of the reaction vertex, and the number of secondary products generated; the following lines give for each secondary product the nature of this product, its mass and atomic numbers, its initial energy just after emission/production, and the Cartesian coordinates of its momentum. In the first line of the database sample shown in **Table 3**, the event #11369 corresponds to a neutron elastic interaction with an As nucleus of the semiconductor lattice, giving a recoil As with an energy of 58 keV.

Table 4 summarizes the main size characteristics of the computed databases for the six semiconductor materials listed in **Table 1** and subjected to 100 million of atmospheric neutrons each. Five size parameters (or metrics) are reported in **Table 4** to quantify the different databases in terms of neutron-semiconductor interactions: the number (fraction) of elastic and inelastic events, the total number of events, the total number of generated secondary products with energy above the energy threshold E_{th} given in **Table 1**, and, finally, the average number of secondary ions produced in the case of inelastic events. **Figures 2** and **3** also graphically represent the fractions of elastic and inelastic events and the total number of interaction events and generated secondary products, respectively. All these results lead to the following remarks:

- Silicon exhibits the lowest total number of interaction events, and, except the particular case of carbon-based materials (diamond and SiC), GaN shows the highest event rate with more than 50% of the supplementary events with respect to Si.
- This result can be explained by the fact that neutron nuclear interaction probability with the elements is even higher than the atomic number Z is. This means that the susceptibility of the materials is all the greater as their atomic number is high [11].

- Diamond shows a very different behavior than the other materials since it is an excellent neutron moderator (better than graphite). This explains the extremely elevated number of elastic events as compared to other materials: ×8 with respect to Ge, ×7 with respect to GaAs, and ×4 with respect to Si.
- Silicon carbide, which can be viewed as a "mixture" of Si and C at the atomic level, shows an intermediate behavior between Si and C with a quasi ×2 number of elastic events due to the presence of C.

Figure 2 shows the fraction of elastic and inelastic events for the different semiconductor materials. We can distinguish three different behaviors with low (< 30%, Ge and GaAs), intermediate

Event Number	**Energy (MeV) of the incident neutron**	**(x, y, z) coordinates of the vertex of the interaction event**			**Number of products**
11369 1	1.938009e+00	-3.123114e+00	2.128556e+00	-2.043811e-03	1
As75[0.0] 75 33	5.865383e-02	4.466775e-01	4.319914e-01	7.834939e-01	
Product	**A Z Energy (MeV)**	**(ux, uy, uz) coordinates of the momentum vector**			
11370 1	2.383369e+02	-1.712552e+00	-2.155406e+00	-2.719637e-03	3
proton 1 1	8.546443e+01	-5.270216e-01	-1.286384e-01	8.400597e-01	
alpha 4 2	1.383653e+01	2.459101e-02	-1.145710e-01	-9.931107e-01	
Ni62[0.0] 62 28	2.160926e+00	8.943092e-02	-1.490662e-01	9.847748e-01	
11371 1	2.638142e+01	-3.206409e+00	-4.575562e+00	9.494563e-03	1
Ga68[0.0] 68 31	6.260841e-01	1.892272e-01	-2.680785e-01	9.446306e-01	
11372 1	2.074821e+02	4.896602e+00	-4.752904e+00	6.255025e-04	2
proton 1 1	1.893323e+02	1.776401e-01	2.641910e-02	9.837408e-01	
Zn68[0.0] 68 30	1.562386e-01	-9.659646e-01	9.698920e-03	2.584925e-01	
11373 1	7.875999e+00	-1.735542e+00	4.719762e+00	-5.800941e-03	1
Ga69[0.0] 69 31	2.959972e-01	3.094430e-02	9.454495e-02	9.950395e-01	
11374 1	1.114444e+02	4.558722e+00	-4.191099e+00	9.470209e-03	2
proton 1 1	6.645712e+00	-4.477549e-01	-6.883188e-01	-5.707301e-01	
Zn64[0.0] 64 30	3.507131e+00	3.622407e-01	1.244171e-01	9.237435e-01	
11375 1	1.541558e+02	2.595860e-01	1.292310e+00	5.783486e-03	2
proton 1 1	3.268971e+01	-3.472904e-02	-3.481138e-01	9.368088e-01	
Ge74[0.0] 74 32	4.819644e-01	-9.020135e-01	3.033525e-01	-3.071628e-01	
11376 1	3.974678e+01	6.775934e-01	4.367106e+00	-9.091089e-03	2
alpha 4 2	7.800831e+00	7.650253e-01	3.799136e-01	5.200019e-01	
Cu64[0.0] 64 29	1.066644e+00	-5.057675e-01	-4.010571e-01	7.637751e-01	
11377 1	2.877963e+02	-1.109289e+00	1.109673e+00	-8.077168e-03	4
proton 1 1	6.803890e+01	2.508779e-01	-6.180162e-01	7.450612e-01	
proton 1 1	1.804781e+01	-3.496855e-01	-7.349503e-01	-5.810061e-01	
deuteron 2 1	1.321282e+01	-5.108815e-01	-4.381425e-01	7.396156e-01	
Zn66[0.0] 66 30	9.454173e-01	9.760912e-01	2.947766e-04	2.173610e-01	

Table 3. Sample (nine events) extracted from the computed database corresponding to GaAs target material subjected to atmospheric neutron irradiation.

Target material	Si	Ge	C (diamond)	4H–SiC	GaN	GaAs
Number of elastic events (fraction, %)	7918 (59.1)	3788 (27.7)	30,536 (79.2)	13,771 (65.1)	8303 (39.1)	4119 (28)
Number of inelastic events (fraction, %)	5482 (40.9)	9898 (72.3)	7981 (20.8)	7390 (34.9)	12,955 (60.9)	10,603 (72)
Total number of events	**13,400**	**13,686**	**38,517**	**21,161**	**21,258**	**14,722**
Total number of secondary products ($E > E_{th}$)	18,989	20,527	48,357	29,067	32,011	21,758
Average number of secondary ions produced in inelastic events	2.02	1.69	2.23	2.07	1.83	1.66

Table 4. Main characteristics of the neutron event databases generated for the six semiconductor materials considered in this work.

(40–60%, Si and GaN), and high (> 60%, C and SiC) elastic event rates; the presence of low-Z elements such as C and N, respectively, in SiC and GaN leads to increase elastic interactions in these last materials with respect to the elastic rates observed for Si and GaAs.

In addition, **Figure 3** shows the total number of interaction events (elastic + inelastic) and the total number of secondary products generated in the different targets. For Si, Ge, and GaAs, this last quantity is in the same order of magnitude (with Si < Ge < GaAs that follows the rule that neutron nuclear interaction probability with the elements is even higher than the atomic number is). For GaN and SiC and as previously mentioned, the presence of low-Z elements, C and N, respectively, increases the number of elastic events and indirectly increases the total number of secondary products. Finally, carbon-diamond material dominates this comparison in terms of the number of events/products due to its high power of neutron moderation.

3.2. Nature of the secondary products

Figure 4 shows the number of events as a function of the number of secondary products generated during the different interaction events. We call this last quantity secondary product

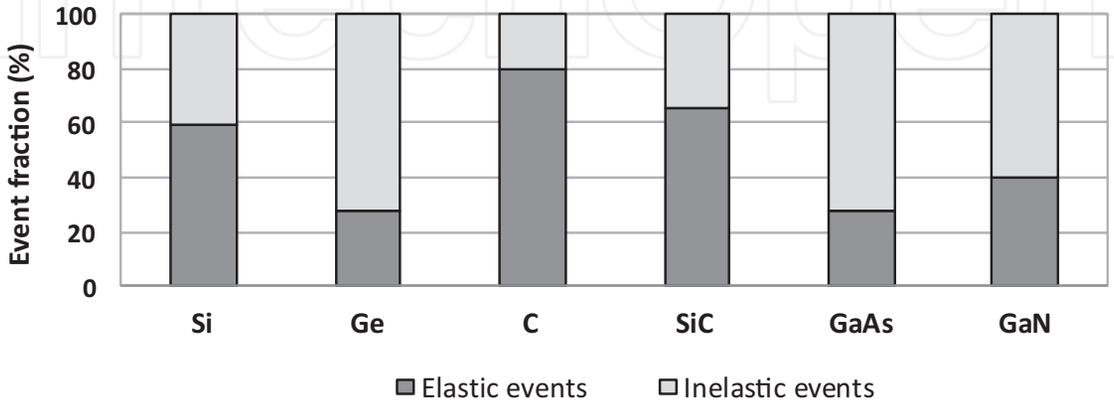

Figure 2. Fraction of elastic and inelastic events for the six semiconductor targets irradiated with atmospheric neutrons.

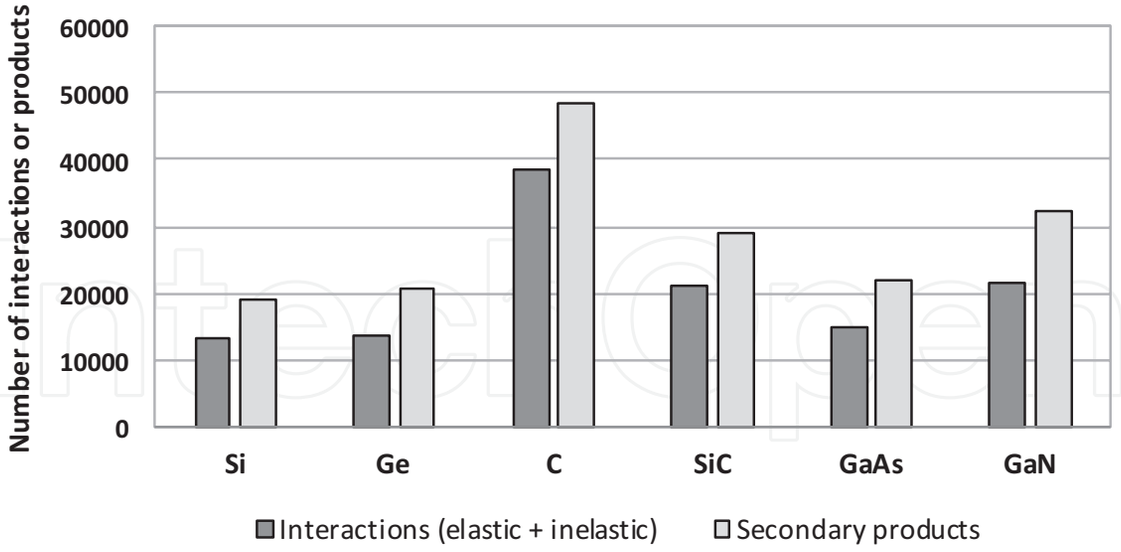

Figure 3. Total numbers of interaction events and secondary products referenced in the different computed databases.

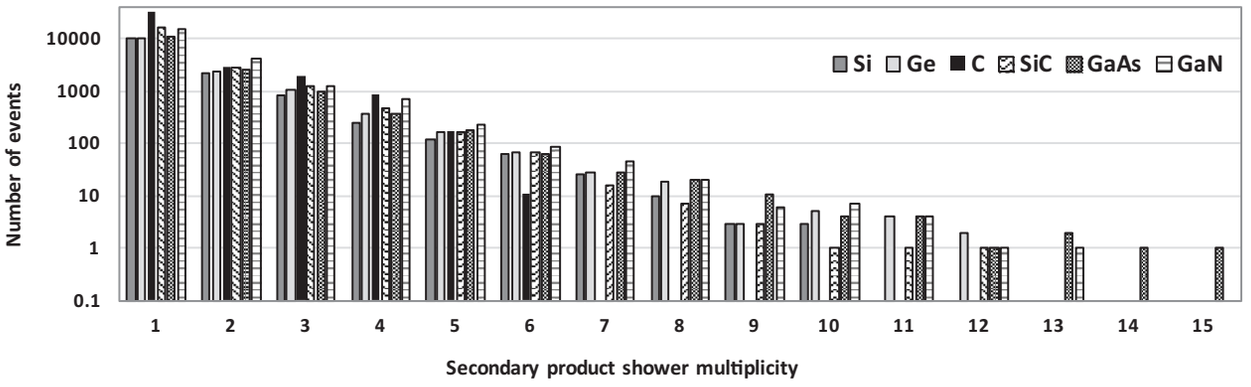

Figure 4. Number of events as a function of the number of secondary products (also called secondary product shower multiplicity) for the six semiconductor materials (for 100 million atmospheric incident neutrons on a volume target of $1cm^2$ x 20 microns).

shower multiplicity (M) because each event can be considered at the origin of a shower of ionizing products: a multiplicity of one (i.e., one product emitted) corresponds to elastic events; larger multiplicities correspond to the production of two or more secondary products during nuclear reactions.

From **Figure 4**, we can formulate the following observations:

- For all targets, the number of reactions monotonously decreases when increasing M. This number of reactions goes to zero above M = 6 for carbon (diamond), M = 10 for silicon, M = 12 for germanium and silicon carbide, M = 13 for gallium nitride, and M = 15 for gallium arsenide.
- For M > 9, the event statistic is therefore relatively weak and may be dependent of the number of incident neutrons. Pushing the statistics beyond 100 million neutrons may give slightly different results for these limits in terms of secondary product shower multiplicity.

- Multi-fragment reactions with M ≥ 4 represent a small but non-negligible part of the events for all semiconductors except for diamond: 3.6% for Si, 4.9% for Ge, 4.6% for GaAs, 5.0% for GaN, and 3.2% for SiC against only 2.8% for C. These large multiplicity events are important because they can produce a single event that potentially impacts several sensitive volumes in a component or a circuit. With respect to silicon, Ge, GaAs, and GaN show a slightly higher probability for such large multiplicity events.

Figures 5 and **6** provide a detailed analysis of the production of these secondary ions, target per target, and as a function of the atomic number of the products. Z is ranging from 1 (proton) to the highest atomic number of the element(s) present in the target material: 6 for carbon, 14 for silicon, 32 for germanium, 31 for GaN, and 33 for GaAs.

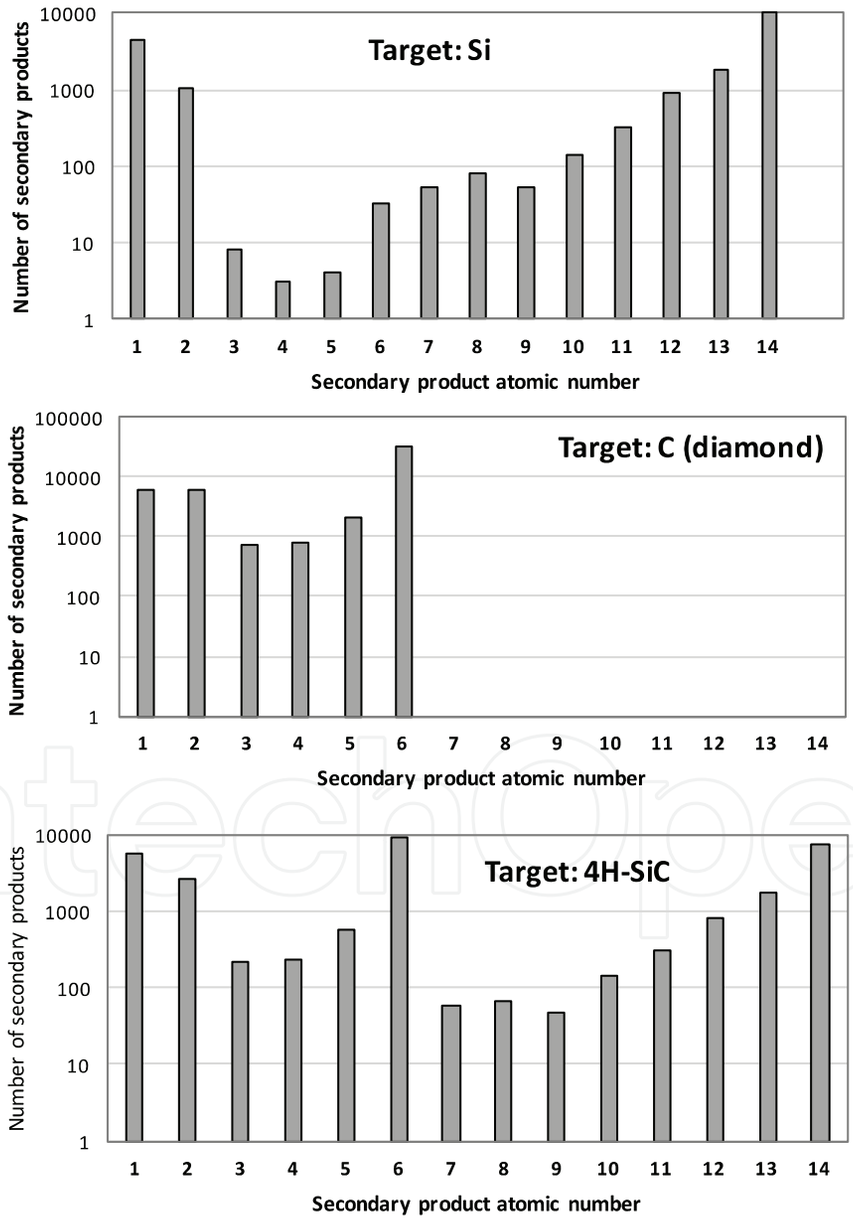

Figure 5. Number of secondary products produced in Si, C (diamond), and SiC as a function of their atomic number (for 100 million atmospheric incident neutrons on a volume target of 1 cm^2 x 20 microns).

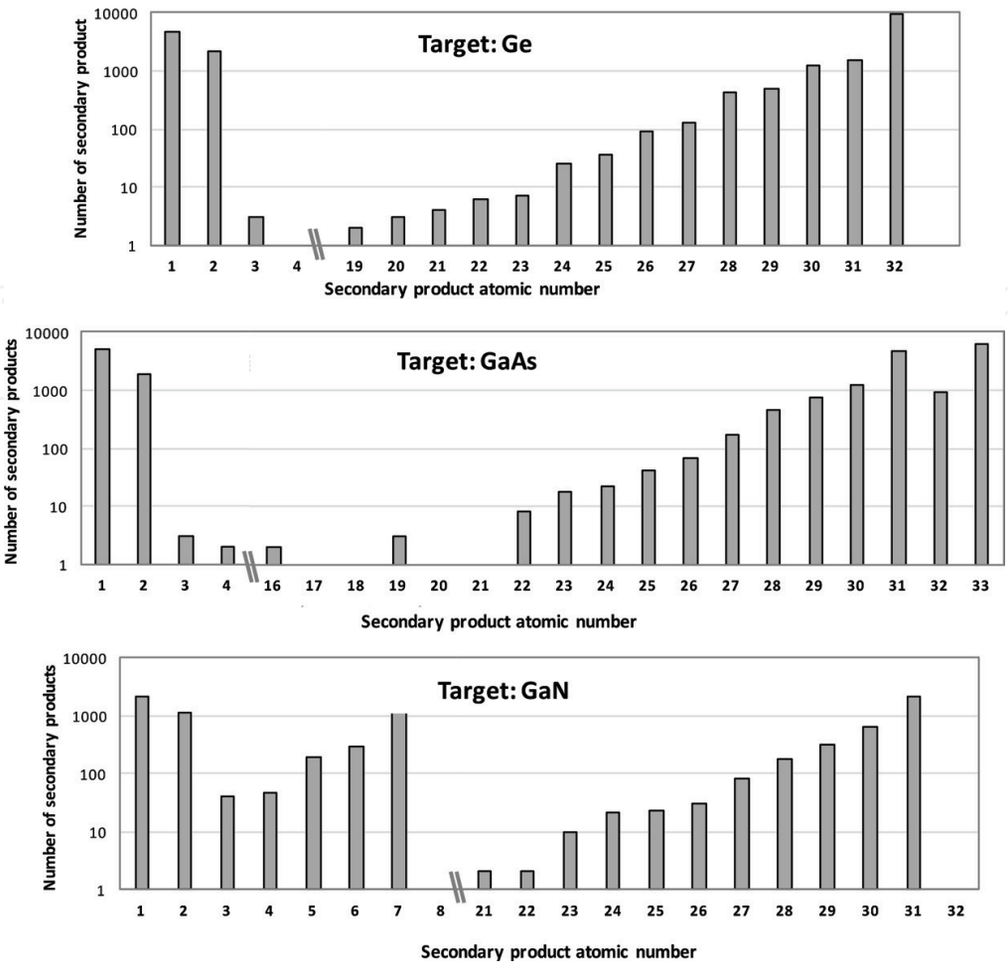

Figure 6. Number of secondary products produced in Ge, GaAs, and GaN as a function of their atomic number (for 100 million atmospheric incident neutrons on a volume target of 1 cm^2 x 20 microns).

For the six materials, the most frequent produced secondary particles are the recoil products due to neutron elastic interactions with the nuclei of the semiconductor lattice, followed by protons in the second position and alpha particles in the third one (in the case of compound materials, recoil nuclei concern the two different species: Si and C recoil products for SiC, Gas and As for GaAs, and Ga and N for GaN). All the other products are systematically less produced than these three categories of products.

This observation justifies why in the following analysis (paragraph 3.3), all produced particles will be divided in four classes: recoil products, protons, alpha particles, and other products.

Also shown in **Figure 5**, beryllium (Z = 4) is the less produced product for silicon target, lithium (Z = 3) for diamond, and fluor (Z = 9) for SiC. Finally, note that in **Figure 6**, an axis-break has been introduced because no secondary product is created between Z = 3 and 19 for Ge, between Z = 4 and 22 (except Z = 16 and 19) for GaAs, and between Z = 7 and 21 for GaN. For these large Z elements (31 for Ga, 32 for Ge, and 33 for As), the absence of fragments in these ranges of Z

http://dx.doi.org/10.5772/intechopen.71528

comes from the limited number of high-energy incident neutrons, due to the 1/E nature of the spectrum of **Figure 1** and to the finite value of the high-energy limit (10^5 MeV) considered for simulation; certain reaction channels being not present in the computed databases.

3.3. Detailed analysis in terms of energy, LET, and range

Figures 7–10 provide a detailed analysis of the secondary ions produced during neutron interactions in the different target materials in terms of initial energy (when products are released), linear energy transfer (LET), and range in the target material.

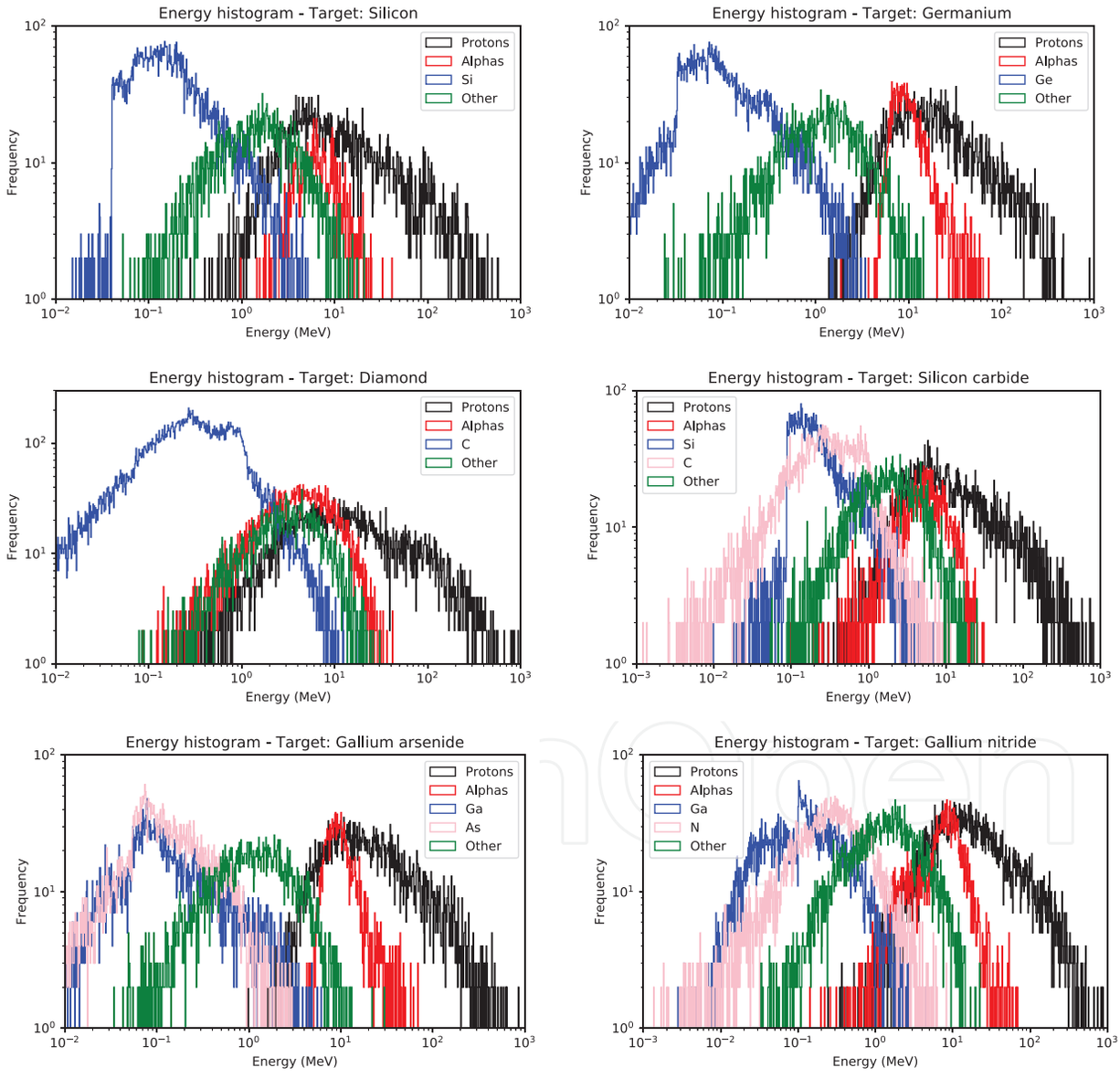

Figure 7. Histograms in energy for recoil nuclei, protons, and alpha particles induced by neutron interactions in the different targets.

LET and range have been obtained from SRIM [12] simulation using numerical functions developed from a behavioral modeling of SRIM Tables [13]. These generalized functions LET(Z, A, E target) and Range(Z, A, E target) have been written in C++ and allow us to calculate the two quantities for any given ion defined by the triplet (Z, A, E energy) and for the semiconductor targets Si, Ge, C, SiC, GaAs, and GaN.

All histograms shown in **Figures 7–10** have been constructed using linear bins with constant bin widths corresponding to the minimum value of the x-axis scale. Curves have been also smoothed in frequency in order to give a more readable aspect to the different distributions.

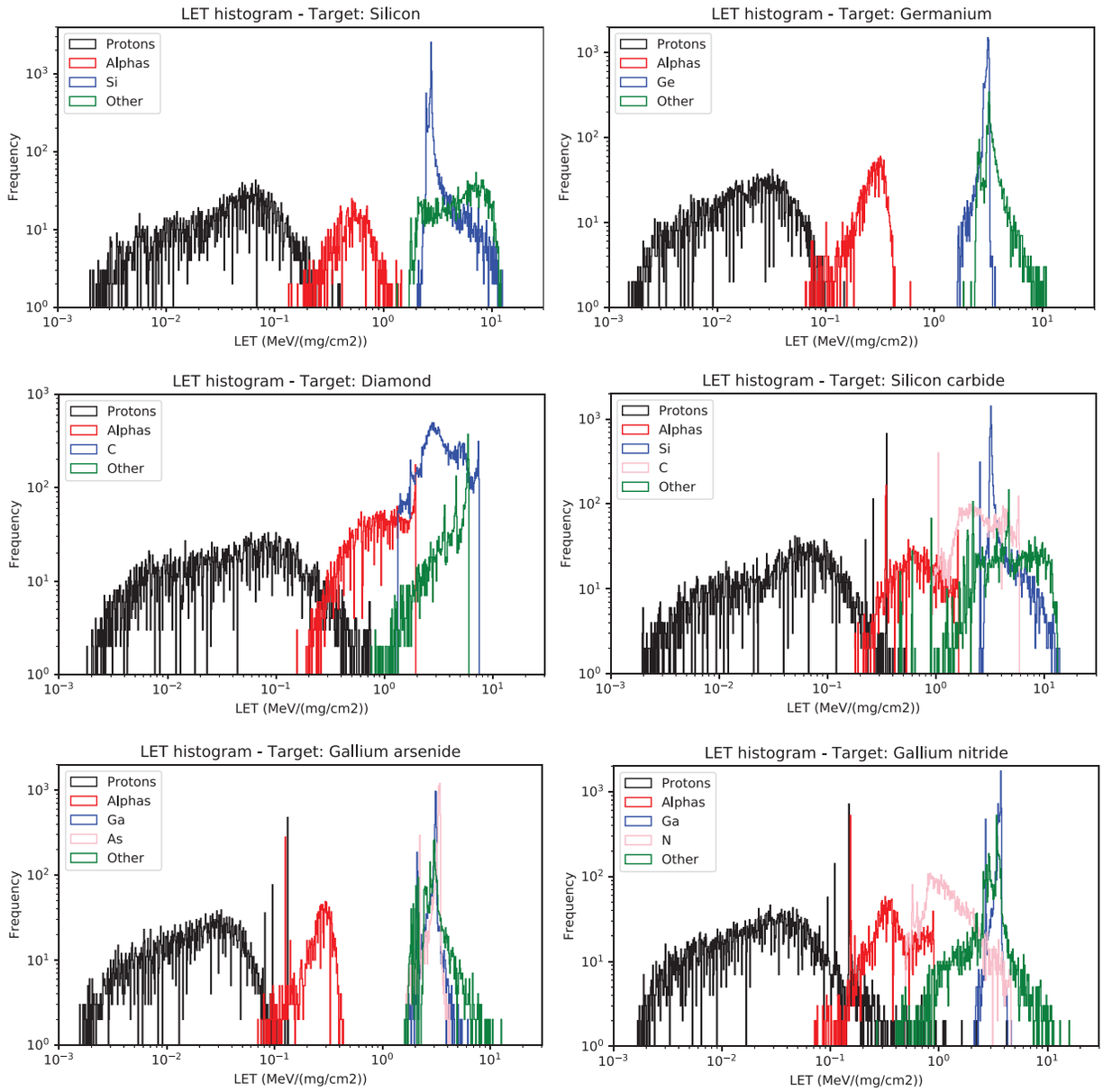

Figure 8. Histograms in LET for recoil nuclei, protons, and alpha particles induced by neutron interactions in the different targets.

http://dx.doi.org/10.5772/intechopen.71528

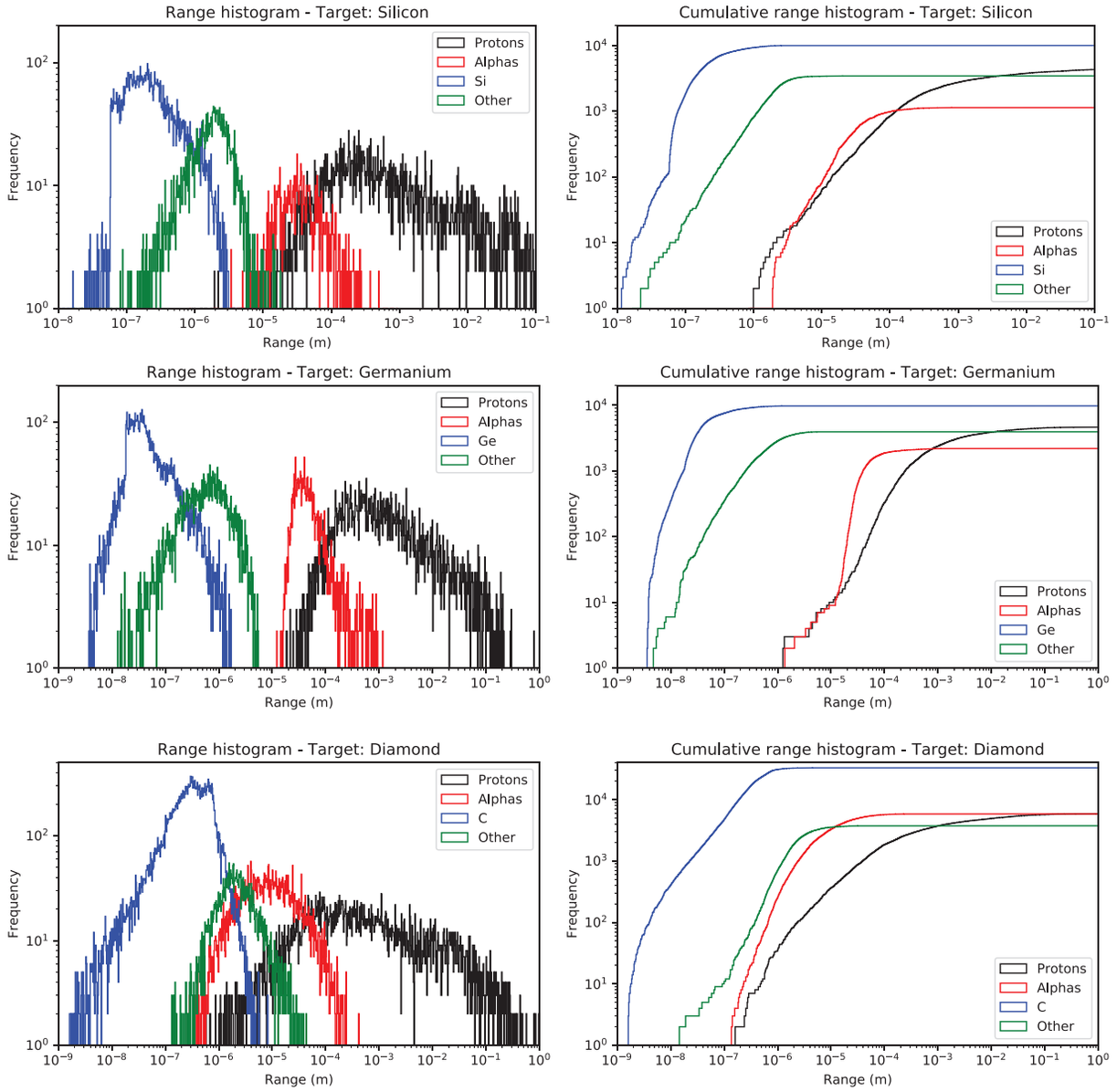

Figure 9. Histograms in range for recoil nuclei, protons, and alpha particles induced by neutron interactions in silicon, germanium, and diamond targets.

Figure 7 shows the histograms in energy for recoil nuclei, protons, and alpha particles induced by neutron interactions in the six targets. We note a certain similarity between the curves related to the different materials:

- Recoil products have systematically a distribution peaking at low energies (1 MeV) and ranging between 1 and 30 MeV for C, 1 and 10 MeV for Si and SiC, 1 to 7–8 MeV for GaAs and GaN, and 1 to 5 MeV for Ge. The high limit in energy of recoil nuclei distributions is much lower than the atomic number Z, which is higher.
- Fragments other than protons and alpha particles show a more broaden distribution than that of recoil products, with a maximum close to 1 MeV and ranging up to a few tens of MeV.

- Alpha particles show a clear peak distribution ranging from 1 MeV to a few tens of MeV and with a maximum around 7–10 MeV, except for C and SiC (around 3 MeV). Above 10 MeV, alpha particles are the most numerous with protons.
- Protons exhibit a large distribution with a maximum around a few MeV (Si, SiC, C) or 10 MeV (Ge, GaAs, GaN) and with a large tail distribution ranging up to several hundreds of MeV (up to 1 GeV for C). Protons clearly dominate in number from 20 MeV to 1 GeV with respect to all other particles.

Figure 8 shows the same data of **Figure 7** but expressed in LET. This transformation has the advantage to show the ionizing power of secondary products just after their release at interaction

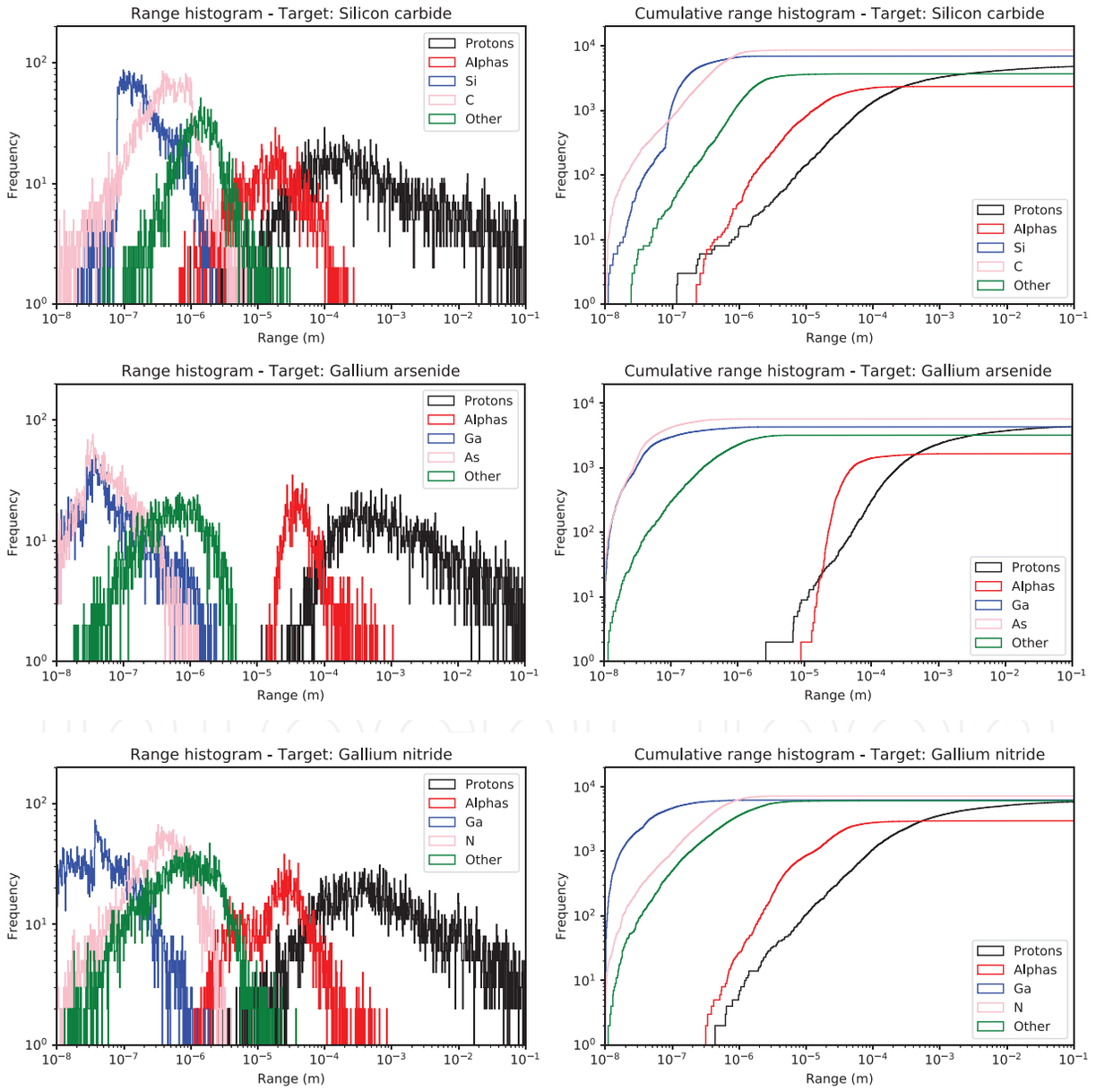

Figure 10. Histograms in range for recoil nuclei, protons, and alpha particles induced by neutron interactions in silicon carbide, gallium arsenide, and gallium nitride targets.

http://dx.doi.org/10.5772/intechopen.71528

vertex position. In the same way as observed in **Figure 7**, distributions of **Figure 8** show similarities from a target to another:

- Heavy products composed of recoil nuclei and fragments other than protons and alpha particles exhibit the highest LET values, in the range 1 to 10 MeV/(mg/cm^2)).
- Recoil product LET values are distributed following a very sharp (peaked) distribution centered at approximately 3 MeV/(mg/cm^2)) for all targets.
- Protons, which are the lightest but the more energetic particles, are characterized by the lowest LET values, from 0.01 to a few 0.1 MeV/(mg/cm^2)).
- Alpha particles exhibit intermediate LET values, with a peak distribution centered in the range 0.1 to a 1 MeV/(mg/cm^2)).

To complete previous results, **Figures 9** and **10** show the range distributions of all products, always partitioned in four classes. On the one hand, recoil and other (heavy) products exhibit the shorter ranges, in the deca-nanometer domain and up to a maximum of a few microns. On the other hand, light products, i.e., protons and alpha particles, show much longer ranges up to a few hundreds of microns for the most energetic alpha particles and ranges up to a few millimeters for high-energy protons.

From results shown in **Figures 8–10**, we can logically conclude that recoil nuclei and heavy fragments other than protons and alpha particles are susceptible to induce single events in a very short range from their emission point and with a relative high efficiency, due to their initial high LET values.

On the contrary, protons and alpha particles are characterized by lower LET values but with longer ranges in the different semiconductor materials. Consequently, they are susceptible to induce single events farther from their emission point than heavy fragments up to distances of hundred microns for alpha particles and several millimeters for protons.

3.4. Consequences in terms of electron-hole pair generation and single events

This last paragraph examines the consequences of neutron interactions in the different targets in terms of electron-hole pair generation and fundamental mechanism at the origin of single events in electronics. From the computed databases, we calculated in **Figure 11** the total energy deposited by all the secondary products in the different target materials. Although it is a purely theoretical value, this total amount of deposited energy by ionization process is in the range of 10^{11} eV for 100 million incident neutrons, which gives an average value in the range of keV per incident neutron, more precisely 1.7 keV for Si, 2.85 keV for Ge, 3.07 keV for C, 2.33 keV for SiC, 2.6 keV for GaAs, and 3.74 keV for GaN. This quantity is found to be minimum for the silicon target and maximum for GaN (**Figure 11**).

Dividing this total energy deposited by all the secondary products by the average energy for creation of an electron-hole pair (given in **Table 1**) gives, for each target material, the upper theoretical limit of the total amount of electron–hole pairs induced by neutrons (via the secondary products). This quantity is shown in **Figure 12** for the different target materials. Also, normalized per incident neutron, this corresponds to 472 e–h pairs for Si, 983 for

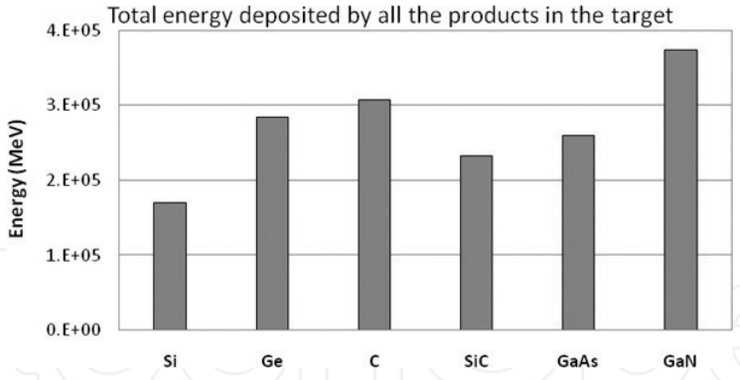

Figure 11. Total energy deposited by all the secondary products induced by neutron interactions in the different target semiconductor materials.

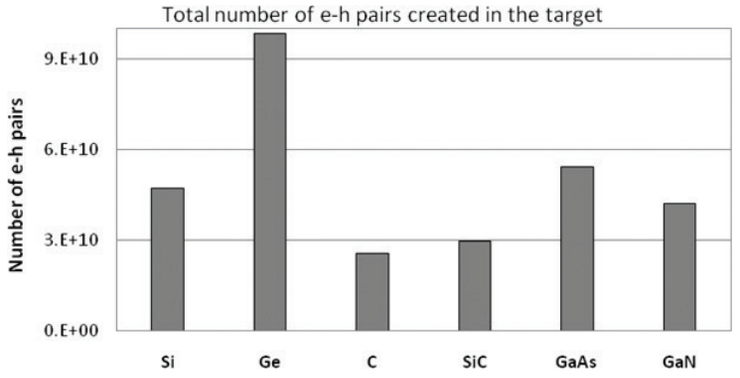

Figure 12. Number of electron-hole pairs created in the different target semiconductor materials by conversion of the total energy deposited by all the secondary products (**Figure 11**), taking into account the average energy for creation of an electron-hole pair given in **Table 1**.

Ge, 256 for C, 299 for SiC, 542 for GaAs, and 420 for GaN. These data show that germanium corresponds to the worst case and diamond (also SiC) to the best case with regard to production mechanisms of single events, Si, GaAs, and GaN being relatively equivalent with respect to this criterion. This result can be for the most part explained by the values of the average energy for creation of an electron–hole pair which is very low for Ge (2.9 eV) and extremely important for C (12 eV).

4. Conclusion

In this chapter, we presented a detailed study using extensive Geant4 numerical simulation of nuclear events resulting from the interaction of atmospheric neutrons at the terrestrial level with a target layer composed of various group-IV and III-V semiconductor materials including silicon, germanium, silicon carbide, carbon-diamond, gallium arsenide, and gallium nitride materials. The neutron interaction responses of these different semiconductors have been finely compared in terms of nuclear processes, recoil products, secondary ion production, and fragment energy distributions. Our results show that Si exhibits the

http://dx.doi.org/10.5772/intechopen.71528

lowest total number of interaction events and, except the particular case of carbon-based materials (diamond and SiC), GaN shows the highest event rate with more than 50% of the supplementary events with respect to Si. Diamond shows a very different behavior than the other materials (our simulation results show a particularly elevated number of elastic events for diamond as compared to other materials) since it is an excellent neutron moderator. For silicon carbide, which can be viewed as a "mixture" of Si and C at the atomic level, it shows an intermediate behavior between Si and C with a number of elastic events quasi ×2 with respect to Si due to the presence of C. Concerning the fraction of elastic and inelastic events, three different behaviors can be highlighted: low (< 30%, Ge and GaAs), intermediate (40–60%, Si and GaN), and high (> 60%, C and SiC) elastic event rates; the presence of low-Z elements such as C and N, respectively, in SiC and GaN leads to increase elastic interactions in these last materials with respect to the elastic rates observed for Si and GaAs. For Si, Ge, and GaAs, the total number of generated secondary products is in the same order of magnitude (with Si < Ge < GaAs). For GaN and SiC, the presence of low-Z elements increases the number of elastic events and indirectly increases the total number of secondary products. Carbon-diamond shows the highest number of events/products due to its high power of neutron moderation. Concerning the nature of the secondary products, our simulations show that, for the six materials, the most frequent produced secondary particles are the recoil products due to neutron elastic interactions with the nuclei of the semiconductor lattice, followed by protons in the second position and alpha particles in the third one. All the other products are systematically less produced than these three categories of products. A detailed analysis of the secondary ions produced during neutron interactions in the different target materials in terms of initial energy (when products are released), linear energy transfer (LET), and range in the target material has been also conducted. Recoil nuclei and heavy fragments have been shown to be susceptible to induce single events in a very short range from their emission point and with a relative high efficiency, due to their initial high LET values. On the contrary, protons and alpha particles, characterized by lower LET values but longer ranges in the different semiconductor materials, are susceptible to induce single events farther from their emission point than heavy fragments up to distances of hundred microns for alpha particles and several millimeters for protons. Finally, the consequences of neutron interactions in the different targets in terms of electron–hole pair generation, a fundamental mechanism at the origin of single events in electronics, have been examined. Our results show that germanium corresponds to the worst case and diamond (also SiC) to the best case with regard to e–h pair production, Si, GaAs, and GaN being relatively equivalent and of intermediate behavior with respect to this criterion.

Author details

Daniela Munteanu and Jean-Luc Autran*

*Address all correspondence to: jean-luc.autran@univ-amu.fr

Aix Marseille Université, CNRS, Université de Toulon, Marseille, France

References

[1] International Techology Roadmap for Semiconductors 2.0. Online available: http://www.itrs2.net

[2] Serre S, Semikh S, Uznanski S, Autran J-L, Munteanu D, et al. Geant4 analysis of n-Si nuclear reactions from different sources of neutrons and its implication on soft-error rate. IEEE Transactions on Nuclear Science. 2012;**59**(4, 1):714-722

[3] Liu H, Cotter M, Datta S, Narayanan V. Technology Assessment of Si and III-V FinFETs and III-V Tunnel FETs from Soft Error Rate Perspective. International Electron Device Meeting, Institute of Electrical and Electronics Engineers. 2012. p. 577-580

[4] Agostinelli S, et al. Geant4 – a simulation toolkit, Nuclear Instruments and Methods in Physics Research Section A: Accelerators, Spectrometers, Detectors and Associated Equipment. 2003;**506**(3):250-303

[5] Allison J, et al. Recent developments in Geant4, Nuclear Instruments and Methods in Physics Research Section A: Accelerators, Spectrometers, Detectors and Associated Equipment. 2016;**835**:186-225

[6] Madelung O. Semiconductors Data Handbook. Berlin Heidelberg; Springer-Verlag. 2004. 691 p

[7] Gordon MS, Goldhagen P, Rodbell KP, Zabel TH, Tang HHK, Clem JM, Bailey P. Measurement of the Flux and Energy Spectrum of Cosmic-Ray Induced Neutrons on the Ground. IEEE Transactions on Nuclear Science. 2004;**51**:3427-3434

[8] Autran JL, Munteanu D. Soft Errors: from particles to circuits. Taylor & Francis/CRC Press. 2015. 439 p

[9] Geant4 General Particle Source (GPS). Online available: https://geant4.web.cern.ch/geant4/UserDocumentation/UsersGuides/ForApplicationDeveloper/html/ch02s07.html

[10] Geant4 version 4.9.4. Online available: http://geant4.cern.ch/collaboration/working_groups/electromagnetic/physlist9.4.shtml

[11] Wrobel F, Gasiot J, Saigné F, Touboul AD. Effects of atmospheric neutrons and natural contamination on advanced microelectronic memories. Applied Physics Letters. 2008. p. 064105

[12] Ziegler JF, Ziegler MD, Biersack JP. SRIM – The stopping and range of ions in matter (2010). Nuclear Instruments and Methods in Physics Research Section B: Beam Interactions with Materials and Atoms. 2010;**268**(11):1818-1823

[13] Martinie S, Saad-Saoud T, Moindjie S, Munteanu D, Autran JL. Behavioral modeling of SRIM tables for numerical simulation, Nuclear Instruments and Methods in Physics Research Section B: Beam Interactions with Materials and Atoms. 2014;**322**:2-6